

# *Arabidopsis* micro-RNA biogenesis through Dicer-like 1 protein functions

Yukio Kurihara and Yuichiro Watanabe<sup>†</sup>

Department of Life Sciences, Graduate School of Arts and Sciences, University of Tokyo, Komaba 3-8-1, Meguro-ku, Tokyo 153-8902, Japan

Edited by Roger N. Beachy, Donald Danforth Plant Science Center, St. Louis, MO, and approved July 12, 2004 (received for review May 3, 2004)

**Micro-RNAs (miRNAs) are small, noncoding RNAs of 18–25 nt in length that negatively regulate their complementary mRNAs at the posttranscriptional level. Previous work has shown that some RNase III-like enzymes such as Droscha and Dicer are known to be involved in miRNA biogenesis in animals. However, the mechanism of plant miRNA biogenesis still remains poorly understood. In this article, the process of *Arabidopsis* miR163 biogenesis was examined. The results revealed that two types of miR163 primary transcripts (pri-miR163s) are transcribed from a single gene by RNA polymerase II and that miR163 biogenesis requires at least three cleavage steps by RNase III-like enzymes at 21-nt-long intervals. The first step is from pri-miR163 to long miR163 precursor (pre-miR163), the second step is from long pre-miR163 to short pre-miR163, and the last step is from short pre-miR163 to mature miR163 and the remnant. It is interesting that, during the process, four small RNAs including miR163 are released. By using *dcl1* mutants, it was demonstrated that *Arabidopsis* Dicer homologue Dicer-like 1 (DCL1) catalyzes at least the first and second cleavage steps and that double-stranded RNA-binding domains of DCL1 are involved in positioning of the cleavage sites. Our result is direct evidence that DCL1 is involved in processing of pri- and pre-miRNA.**

**M**icro-RNAs (miRNAs) are endogenous, small, noncoding RNAs of 18–25 nt in length that negatively regulate their complementary mRNAs at the posttranscriptional level in many eukaryotic organisms (1). A large number of miRNAs have been discovered in both plants and animals (2–4).

In animals, especially in the human, miRNA biogenesis and functional pathways have been examined and partly described. First, miRNA primary transcripts (pri-miRNAs) are trimmed in the nucleus into miRNA precursors (pre-miRNAs) by an RNase III-like enzyme called Droscha (5). After this initial processing, the pre-miRNAs are exported to the cytoplasm by the function of exportin-5 (6, 7) and are cleaved there to generate mature miRNAs by another RNase III-like enzyme called Dicer (8).

These miRNAs are then incorporated into the RNA-induced silencing complex (RISC) endonuclease, which seems to negatively regulate the genes required for several developmental processes by promoting RISC-mediated degradation of target mRNAs, or the inhibition of target mRNA translation (9).

In the genome of *Arabidopsis thaliana*, four Dicer-like (DCL) enzymes (DCL1–DCL4) are encoded (10). It has been shown that one of the enzymes, DCL1, is involved in miRNA accumulation (11). It is also known that DCL1 mRNA is subject to negative feedback regulation by miR162-guided mRNA degradation (12). On the other hand, DCL2 and DCL3 proteins are partly involved in viral short interfering RNA (siRNA) biogenesis and endogenous siRNA biogenesis such as retrotransposon siRNA, respectively (13).

However, the mechanism of plant miRNA biogenesis, including the step where DCL1 acts, remains poorly understood, because it has been difficult to detect pri- and pre-miRNAs by Northern blot analysis. Here we report that miR163 biogenesis requires at least three cleavage steps by RNase III-like enzymes and that DCL1 catalyzes at least the first and second cleavage step. We also show that double-stranded RNA

(dsRNA)-binding domains of DCL1 are involved in positioning of the cleavage sites.

## Materials and Methods

**Plant Materials.** Plant growth conditions were as described (14) and differed only in photoperiod length, which was 16 h/8 h in this study. *DCL1-9/DCL1-9* homozygous plants were distinguished from *DCL1-9/dcl1-9* heterozygous plants by PCR amplification of the octopine synthase terminator sequence of the T-DNA (portion of the tumor-inducing plasmid that is transferred to plant cells) by using genomic DNA as a template and the primers 5'-CTCCGTTCAATTTACTGATTGTAC-3' and 5'-TTGAATGGTGCCCCGTAACCTTTTCG-3'.

**Northern Blot Analysis.** Total RNA was extracted from the entire aerial portions of plants inoculated with mock or crucifer tobamovirus Cg (TMV-Cg) (14) by using TRIzol reagent (Invitrogen). Low molecular weight RNA plus (LMW RNA+) was isolated by anion-exchange chromatography (RNA/DNA Midi kit, Qiagen, Valencia, CA) according to the manufacturer's instructions with a minor exception: a specific elution buffer [50 mM Mops/1.0 M NaCl, pH 7.0/15% (vol/vol) ethanol] was used in the elution step. For detection of pri-miR163, pre-miR163, and miR163, LMW RNA+ was resolved with electrophoresis on a denaturing 5% polyacrylamide gel (8 M urea) and 15% polyacrylamide gel (7 M urea), respectively, in 0.5× TBE buffer (89 mM Tris/89 mM boric acid/2 mM EDTA, pH 8.3) and electroblotted onto Hybond-N<sup>+</sup> membranes (Amersham Pharmacia). Radiolabeled DNA probes (probes 1 and 2) were constructed by random priming reactions in the presence of [ $\alpha$ -<sup>32</sup>P]dCTP by using the Megaprime DNA-labeling system (Amersham Pharmacia). Radiolabeled DNA oligonucleotide probes were constructed by end-labeling with [ $\gamma$ -<sup>32</sup>P]ATP by using T4 polynucleotide kinase. Two probes, 1 and 2, contained the following sequences, with nucleotide numbers starting at the beginning of the pri-miR163: nucleotides 149–479 (probe 1) and nucleotides 1–146 (probe 2). Probes 3 and 4 were end-labeled DNA oligonucleotides: 5'-ATCGAAGTTCCAAGTCTCTTCAA-3' (probe 3) and 5'-CGATTTTATCCAAAGGGTTTTGGT-3' (probe 4). Probe 1' contained the region of *DCL1-9* pre-miR163 corresponding to probe 1. The probes for detection of upper-left (UL), miR163\*, and lower-left (LL) small RNAs were also end-labeled DNA oligonucleotides that were complementary to their respective sequences.

This paper was submitted directly (Track II) to the PNAS office.

Abbreviations: miRNA, micro-RNA; pri-miRNA, miRNA primary transcript; pre-miRNA, miRNA precursor; DCL, Dicer-like; dsRNA, double-stranded RNA; T-DNA, portion of the tumor-inducing plasmid that is transferred to plant cells; TMV-Cg, tobamovirus Cg; Ler, *Landsberg erecta*.

Data deposition: The sequences reported in this paper have been deposited in the GenBank database [accession nos. AY615373 (pri-miR163 sequence type 1) and AY615374 (pri-miR163 sequence type 2)].

<sup>†</sup>To whom correspondence should be addressed. E-mail: solan@bio.c.u-tokyo.ac.jp.

© 2004 by The National Academy of Sciences of the USA

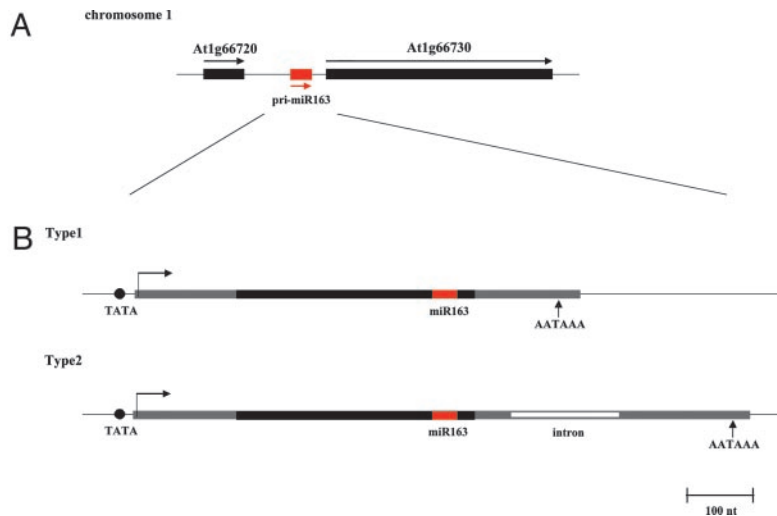


**Fig. 1.** Localization and sequence of the miR163 gene. (A) The miR163 gene is located on chromosome 1 between the At1g66720 and At1g66730 genes. The red box indicates the miR163 gene, and the black boxes indicate two adjacent genes. (B) Schematic representation of miR163 gene organization. Bold black lines and red lines indicate the sequences corresponding to the stem-loop-forming region of primary transcript (pri-miR163) and miR163, respectively. The positions of the polyadenylation signal (AATAAA) are pointed to by arrows. It was thought that type 2 pri-miR163 could emerge by splicing through exclusion of the polyadenylation signal for type 1 pri-miR163.

**Mapping of pri-miR163 Sequence.** For mapping of the pri-miR163 sequence, RNA ligase-mediated rapid amplification of cDNA ends was performed by using the GeneRacer kit (Invitrogen) according to the manufacturer's instructions. Total RNA was extracted from whole *Arabidopsis* plants. Poly(A)<sup>+</sup> RNA was purified by using the Oligotex-dT30 Super mRNA-purification kit (Takara) and ligated to the GeneRacer RNA oligo adapter (5'-CGACUGGAGCACGAGGACACUGACAUGGACUGAAGGAGUAGAAA-3'). The GeneRacer Oligo(dT) primer [5'-GCTGTCAACGATACGCTACGTAACGGCATGACAGTG(T)<sub>18</sub>-3'] was then used to prime first-strand cDNA synthesis in the reverse-transcription reaction. The 5' ends of pri-miR163 cDNA were amplified with the GeneRacer 5' primer (5'-CGACTGGAGCACGAGGACACTGA-3') and gene-specific primer (5'-ACACGGGGGATAATATCGAA-3'). The 3' ends were amplified with the GeneRacer 3' primer (5'-GCTGTCAACGATACGCTACGTAACG-3'), GeneRacer 3' nested primer (5'-CGCTACGTAACGGCATGACAGTG-3'), and gene-specific primer (5'-ACCCGGTGGATAAAATC-GAG-3'). PCR products were gel-purified and cloned into pCR2.1 TOPO vector (Invitrogen) for sequencing.

**Determination of Cleavage-Site Sequence.** Aliquots of 5 μg of low molecular weight RNA plus were self-ligated with T4 RNA ligase; the reaction volume was 100 μl, and the reaction was performed overnight at 14°C. After the ligation reaction, RNAs were phenol/chloroform-extracted and precipitated with ethanol, and pre-miR163s or remnants were amplified by RT-PCR with the gene-specific primers 5'-GAAGTAACGCGCAGTGCTTA-3' and 5'-ACCGTGCTCTTCCTAA-GAAG-3', which were used in both the reverse-transcription reaction and PCR. These two primers have sequences corresponding to nucleotides 375–394 (antisense) and 399–419 (sense) of pri-miR163, respectively. PCR products were gel-purified and cloned into pCR2.1 TOPO vector for sequencing.

**Prediction of RNA Secondary Structure.** The potential secondary structures of pre-miR163 were predicted by using MFOLD 3.1 (<http://molbio.info.nih.gov/molbio-nih/mfold.html>).

## Results and Discussion

**Characterization of pri-miR163.** Most of the genes coding miRNA sequences are located in intergenic regions of the genome. In

the *Arabidopsis* genome, the miR163 gene is located on chromosome 1 between the At1g66720 and At1g66730 genes (Fig. 1A). We discovered that both pri-miR163 and pre-miR163 could be detected easily (unpublished data; Fig. 2). To examine the detailed process of miRNA biogenesis, we first determined the full sequence of pri-miR163 by 5' and 3' rapid amplification of cDNA ends methods using oligo(dT) primers. Interestingly, we obtained two types (types 1 and 2) of pri-miR163 sequences [GenBank accession nos. AY615373 (type 1) and AY615374 (type 2)] (Fig. 1B). Both have a polyadenylation signal, but type 2 has an intron bearing exact splice sites. Because the polyadenylation signal of type 1 was located in the intron of type 2, it was thought that type 2 pri-miR163 emerged by splicing through exclusion of the polyadenylation signal for type 1 pri-miR163. Another possible polyadenylation signal for type 2 pri-miR163 was found downstream from the intron. In addition, we could find a TATA box-like sequence upstream from the transcribed region. Taken together, it is obvious that pri-miR163 is transcribed by RNA polymerase II.

**miR163 Biogenesis Requires at Least Three Cleavage Steps.** We performed Northern blot analysis by using a probe complementary to the putative stem-loop region (Fig. 2A, probe 1) and then detected some species of RNAs in uninfected (mock) and TMV-Cg-infected plants. TMV-Cg infection could increase accumulation of most miRNAs (unpublished data). Previous work showed that expression of viral suppressors of RNA silencing increased miRNA accumulation (15–17). We preferentially used a TMV-Cg-infection condition for this Northern blot analysis, because it dramatically increased the accumulation of band d, described below, as well as miR163. Judging from the molecular lengths, it was assumed that bands a, c, and d correspond to pri-miR163, pre-miR163, and remnant after release of mature miR163, respectively. Band b probably corresponds to the precursor of pre-miR163. To confirm our assignments, we used three other probes (probes 2–4) that are complementary to the 5' end sequence of pri-miR163, the 24-nt miR163 sequence, and the stem root of pri-miR163 (Fig. 2A). Probe 2 detected band a and new reproducible band e, probe 3 detected bands a–c, and probe 4

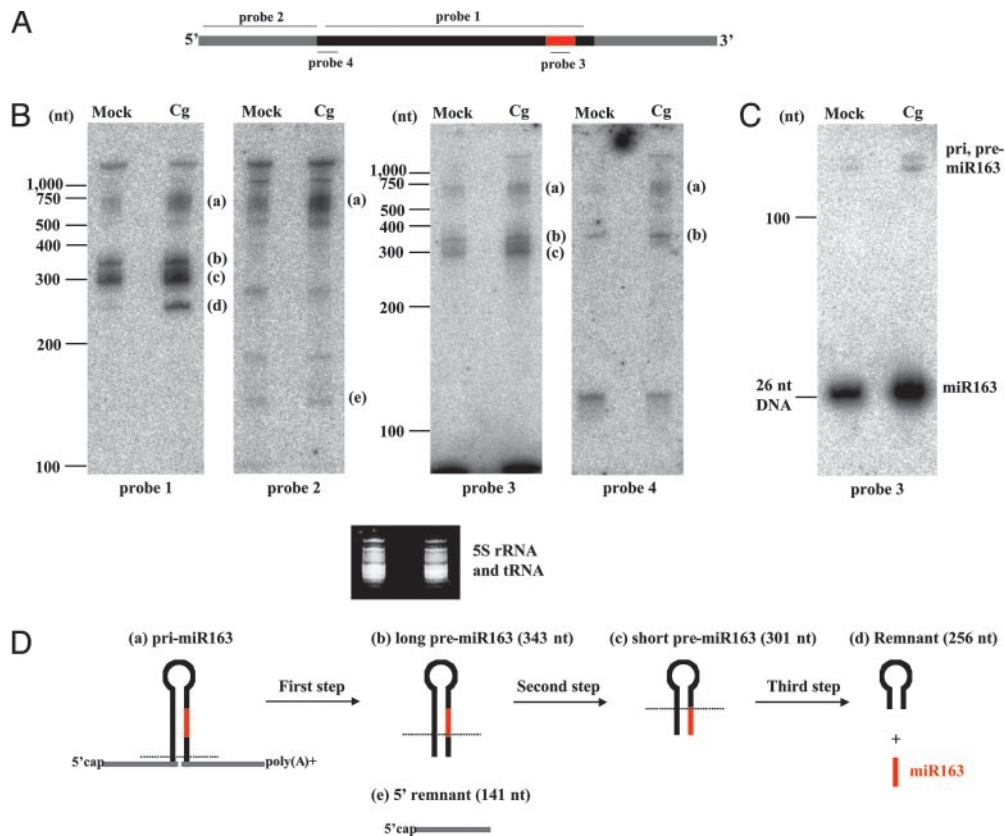


**Fig. 2.** miR163 biogenesis requires at least three cleavage steps. (A) Positions of the four probes used in this study. Bold black lines and red lines indicate the sequences corresponding to the stem-loop-forming region of pri-miR163 and miR163, respectively. (B) Northern blot analysis for detection of pri-miR163 and/or pre-miR163s using the four kinds of probes shown in A. Size markers (Ambion, Austin, TX) are indicated to the left of each panel. Bands a–e correspond to those shown in the model (D). (C) Northern blot analysis for detection of miR163. Positions of the 26-nt DNA oligonucleotide and 100-nt RNA are indicated to the left. The image of 5S rRNA and tRNA was used as a loading control for both B and C. Samples were isolated from uninfected (mock) and TMV-Cg-infected (Cg) plants 10 days after inoculation. (D) Model of miR163 biogenesis. The pri-miR163 (a) is processed into long pre-miR163 (b) at the root of the stem-loop structure, releasing 5' remnant (e). At the next step, long pre-miR163 is cleaved into short pre-miR163 (c) at the edge of the miR163 sequence (second step). Last, short pre-miR163 is cleaved at the opposite edge of the miR163 sequence, producing mature miR163 and remnant (d). The predicted molecular length of each RNA from the result of Fig. 3C is shown in this model.

detected bands a and b (Fig. 2B, probes 2–4) as expected. Fig. 2C shows detection of mature miR163 using probe 3.

Based on the results shown in Fig. 2B and C, we suggest a model for miR163 biogenesis (Fig. 2D). The pri-miR163 (a) is processed into long pre-miR163 (b) at the root of the stem-loop structure, releasing 5' remnant (e), which corresponds to 5' end of pri-miR163 (first step). At the next step, long pre-miR163 is cleaved into short pre-miR163 (c) at the edge of the miR163 sequence (second step). Last, short pre-miR163 is cleaved at the opposite edge of the miR163 sequence, producing mature miR163 and remnant (d) (third step). Thus, miR163 biogenesis requires at least three cleavage steps, probably by RNase III-like enzymes.

**Determination of Positions and Forms of RNase III-Cleavage Sites.** To determine the forms of three cleavage sites and confirm whether they are catalyzed by RNase III proteins, we used a method described previously (18). RNAs were self-ligated, followed by RT-PCR using gene-specific primers (Fig. 3A). Three bands detected between 200- and 400-nt molecular markers were cloned and sequenced (Fig. 3B). The result is shown in Fig. 3C. All three identified cleavage sites had a 3' overhang of 2 or 3 nt, which is a feature of RNase III cleavage (Fig. 3C). It is notable that the length of two intervals between separate cleavage sites was 21 nt long if a few bulges were not counted. These intervals indicate that any DCL proteins that

are involved in miRNA biogenesis probably measure  $\approx 21$  nt in length from one end to the next cleavage site, and then the site was processed. This hypothesis is parallel with a previously proposed cleavage model of animal Dicer (19). Our result also suggested that the enzyme measures 21 nt on one strand of the duplex RNA, because the miR163 strand is actually 24 nt in length, whereas the other strand is 21 nt (Fig. 3C, gray box).

From this result, it was suspected that the other three cleavage products [which we named upper left (UL), lower left (LL), and miR163\*, respectively; Fig. 3C] might be miRNAs. Therefore, we performed Northern blot analysis for detection of these products and miR163 by using probes complementary to them. Small RNA UL and miR163 were detected easily, but small RNA LL and miR163\* were not detected easily (Fig. 3D). We noticed that small RNA UL was identical to small RNA 91, which has been designated already (3). Thus, the small RNA UL (or 91) could be a candidate for miRNA. However, we could not discover complementary target mRNAs to small RNA UL by using the conventional BLAST method, probably because of lower complementarity.

**Disruption of miR163 Biogenesis in *dcl1* Mutants.** miR163 biogenesis in *dcl1-7* [*sin1-1*; Landsberg *erecta* (Ler) background] and *dcl1-9* (*carpel factory*) mutants were examined by Northern blot analysis. The *dcl1-7* mutant carries an amino acid substitution

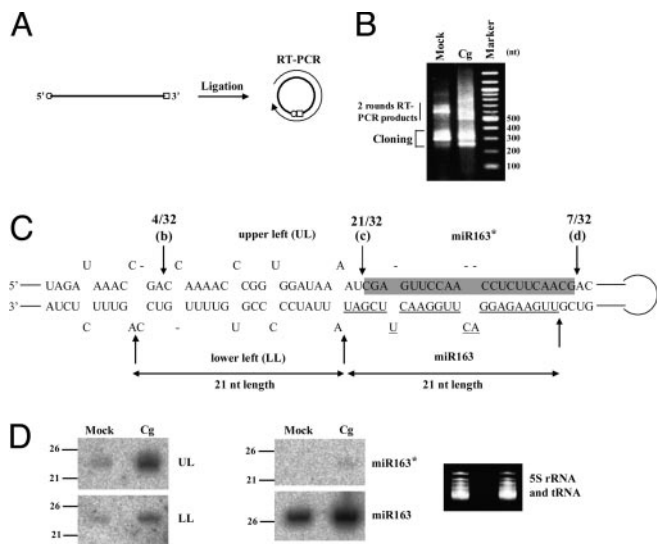


**Fig. 3.** Determination of positions and forms of RNase III-cleavage sites. (A) Illustration of the method used in this study. RNAs were self-ligated, followed by RT-PCR using miR163 gene-specific primers. (B) Image of agarose gel electrophoresis of RT-PCR products. Three bands detected between 200- and 400-nt molecular markers were cloned and sequenced. Bands at a higher molecular weight position were from two rounds of RT-PCR products. (C) Sequence of the stem region of pri-miR163. The three cleavage sites are indicated by arrows b–d, which correspond to the roots of structures b–d shown in Fig. 2D. The number of sequenced clones corresponding to each site is indicated above each cleavage site. The sequence of miR163 is underlined. The gray box indicates the 21-nt-long miR163\*, the opposite strand from miR163. Three kinds of small RNAs produced by the three cleavage steps were designated as upper left (UL), lower left (LL), and miR163\*, respectively. (D) Northern blot analysis for detection of four kinds of small RNAs shown in C. The positions of the 21- and 26-nt oligonucleotides are indicated in *Left* and *Center*. The image of 5S rRNA and tRNA was used as a loading control.

(P415S) in the RNA helicase domain of the DCL1 protein (10, 20), whereas the *dcl1-9* mutant has a T-DNA insertion in the coding region for a second dsRNA-binding domain of DCL1 protein (10, 21). Both mutants fail to accumulate miRNAs (11, 16, 22). First, we performed Northern blot analysis by using probe 1 (shown in Fig. 2A). In *dcl1-7* mutants, the accumulation of long pre-miR163 was at a similar level to that seen in wild-type Ler plants (Fig. 4A, band b), whereas the accumulation of short pre-miR163 and miR163 were at lower levels than those seen in wild-type plants (Fig. 4A, band c). When the accumulation levels of band b were normalized to 1.0 and the relative digital density of band c was evaluated, the c/b ratio in the case of *dcl1-7* was lower than that seen in the case of wild-type Ler (Fig. 4A, under the panels).

The background in *DCL1-9* plants was not wild-type Ler (at least with respect to the miR163 gene). The pri-miR163 gene in the *DCL1-9* plants had an unexpected 12-nt deletion and 60-nt insertion in the loop-forming region of its transcript (Fig. 6, which is published as supporting information on the PNAS web site), although the structure of the stem-forming region of pre-miR163s was completely the same. Therefore, the molecular length of long pre-miR163, short pre-miR163, and the remnant should be 48 nt longer than those of Col-0 or Ler plants. In *dcl1-9/dcl1-9* homozygous mutants, the accumulation of short pre-miR163 was at a lower level than that seen in *DCL1-9/DCL1-9* homozygous or *DCL1-9/dcl1-9* heterozygous plants (Fig. 4B, band g), whereas the accumulation of long pre-miR163 was at a similar level to that seen in *DCL1-9/DCL1-9* or *DCL1-9/dcl1-9* plants (Fig. 4B, band f). The g/f ratio was also lower than that of *DCL1-9/DCL1-9* and *DCL1-9/dcl1-9* plants

(Fig. 4B, under the panels). These results indicate that DCL1 catalyzes at least the second cleavage step from long pre-miR163 to short pre-miR163.

Next, we performed Northern blot analysis by using probe 2 (shown in Fig. 2A). In *dcl1-7* mutants, the 5' remnant released after the first cleavage step was not detected (Fig. 4C, band e), and the accumulation of pri-miR163 increased (Fig. 4C, band a). This result indicates that DCL1 also catalyzes the first cleavage step from pri-miR163 to long pre-miR163. In all *DCL1-9/DCL1-9*, *DCL1-9/dcl1-9*, and *dcl1-9/dcl1-9* backgrounds, the bands corresponding to the 5' remnant were not detected (data not shown).

Previous work showed that in both *dcl2* and *dcl3* mutant plants, the accumulation of miRNAs was not affected compared with wild-type plants (13). We examined whether the defects in *dcl2* and *dcl3* mutants could affect miR163 biogenesis. The *dcl2-2* (SALK\_123586) and *dcl3-1* (SALK\_005512) mutants contain T-DNA insertions in the *DCL2* (At3g03300) and *DCL3* (At3g43920) genes, respectively. Accumulation of all miR163-related RNAs, including miR163 itself, was not affected in *dcl2-2* and *dcl3-1* mutants (Fig. 4D).

**Aberrant Positioning of Cleavage Sites in the *dcl1-9* Mutant.** We examined the forms of three cleavage sites of miR163 and its precursors in *dcl* mutant backgrounds in the same way as described above. As shown in Fig. 5A, in *dcl1-7* and *dcl1-9/dcl1-9* mutants, RT-PCR products had a relatively slow mobility compared with that of the wild type (Ler or *DCL1-9/DCL1-9*). This result was consistent with the results shown in Fig. 4A and B, in which the accumulation of lower molecular RNA species (short pre-miR163 and remnant) was lower than that of the wild type (Fig. 4A and B).

We performed cloning and sequencing of the RT-PCR products from *dcl1-7*, *dcl1-9/dcl1-9*, *DCL1-9/DCL1-9*, *dcl2-2*, and *dcl3-1* mutants. Three cleavage sites were consistent (as shown in Fig. 3C) among *dcl1-7*, *DCL1-9/DCL1-9*, *dcl2-2*, and *dcl3-1* mutants (data not shown), whereas the cleavage sites were different in *dcl1-9/dcl1-9* mutants. The result of the *dcl1-9/dcl1-9* mutant is shown in Fig. 5B. Cleavage sites were not strictly identical or mapped within 4–5 nt as depicted in Fig. 5B (expressed in the gray zones). The first cleavage site was mapped within zone f (Fig. 5B), and the second cleavage site was within zone g. Both sites shifted to the loop side compared with those of the *DCL1-9/DCL1-9* plant. It is interesting that the length of the interval between these two cleavage sites is  $\approx 21$  nt long. It was thought that *dcl1-9* protein could not process the regular cleavage position(s) because of its disrupted second dsRNA-binding domain. Therefore, dsRNA-binding domains of DCL1 protein have an important role in determination of the cleavage positions. We sequenced 30 clones, but the third cleavage site was not identified, probably because the position of the 21-nt sequence from the second cleavage site was not in the dsRNA-forming region.

Taken together with the results shown in Fig. 4, this result in *dcl1-9* mutants suggests that DCL1 catalyzes at least the first and second cleavage steps.

**miRNA Biogenesis in Plants.** In this article we investigated detailed miR163 biogenesis, which is mediated through Dicer-like1 protein functions. Our data indicate that DCL1 not only catalyzes at least the first cleavage step from pri-miR163 to long pre-miR163 and the second cleavage step from long pre-miR163 to short pre-miR163, releasing another miRNA candidate, small RNA UL, but also is involved in positioning of the cleavage sites. We also suspected that the third cleavage step might be catalyzed by DCL1. Therefore, it is suggested that all cleavage steps are probably catalyzed by the DCL1 protein. Thus, miR163 biogen-

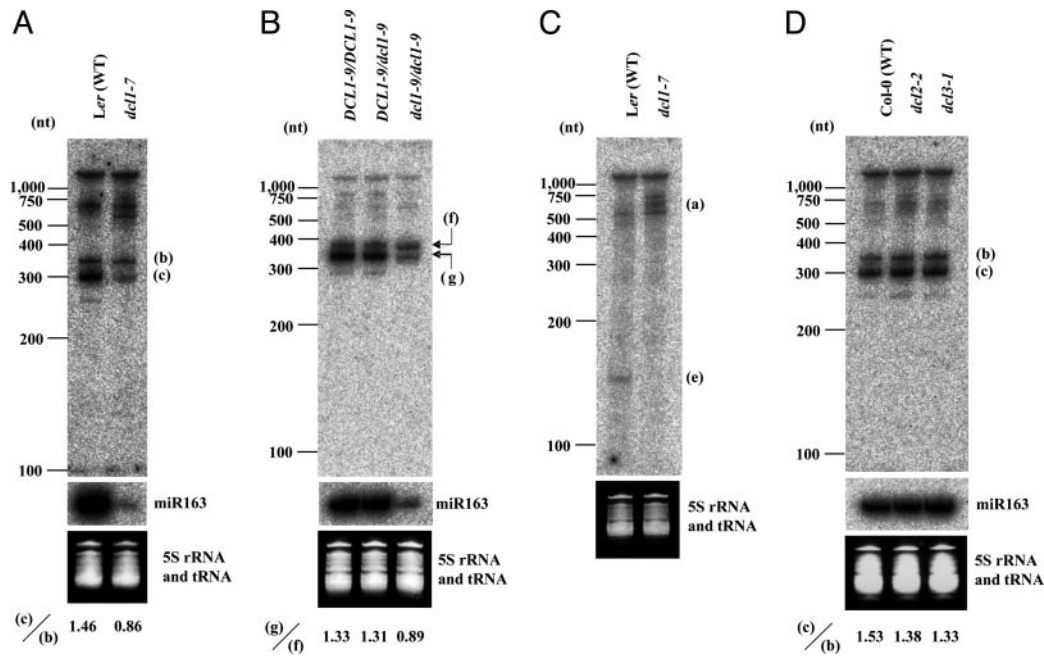


**Fig. 4.** miR163 biogenesis in *dcl* mutants. (A) Northern blot analysis for detection of pri-miR163 and pre-miR163 in *dcl1-7* mutants using probe 1 (shown in Fig. 2A). (B) Northern blot analysis for detection of pri-miR163 and pre-miR163 in *dcl1-9* mutants using probe 1', which covers the stem-loop-forming region of DCL1-9 pri-miR163. (C) Northern blot analysis for detection of pri-miR163 and 5' remnant in *dcl1-7* mutants using probe 2 (shown in Fig. 2A). (D) Northern blot analysis for detection of pri-miR163 and pre-miR163 in *dcl2-2* and *dcl3-1* plants. miR163 was detected by using probe 3 (shown in Fig. 2A). The image of 5S rRNA and tRNA was used as a loading control.

esis is a powerful tool to investigate plant miRNA-maturation processes.

miR163 biogenesis requires three cleavage steps by RNase III-like enzymes. Because the dsRNA-forming stem regions of most of the other predicted pre-miRNAs in *Arabidopsis* were much shorter than that of pre-miR163, and they do not have the two 21-nt-length sequences, it is supposed that most plant miRNA biogenesis generally requires only two cleavage steps, from pri-miRNA to pre-miRNA and from pre-miRNA to the remnant and miRNA.

Previous work has shown that pre-miR167 is found in the

nucleus but not in the cytoplasm, whereas mature miR167 is found in the cytoplasm but not in the nucleus in the tomatoes (23). It has also been shown that *Arabidopsis* DCL1 protein contains two putative nuclear localization signals (NLSs) (10) and partial DCL1 (including NLSs); green fluorescent protein fusion proteins localize to nuclei in the onion cells (24). Taken together, our results suggest that all processes of plant miRNA biogenesis occur in the nuclei.

In animal miRNA biogenesis, the first cleavage step from pri-miRNA to pre-miRNA is catalyzed by an RNase III enzyme, Drosha, but not Dicer (5). However, whole-genome analysis suggested that the *Arabidopsis* genome does not encode a Drosha homologue. In *Arabidopsis*, our data suggest that the Dicer homologue DCL1 has a Drosha function to catalyze the first cleavage step as well as a Dicer function. In addition, plant pre-miRNAs are usually much longer than those of animals. These differences between plant and animal miRNA biogenesis are very interesting, although it is unknown why they occur.

It was shown that dsRNA-binding domains of DCL1 protein have an important role in determination of the first and second cleavage positions (Fig. 5B). However, it was observed that the 21-nt interval between the first and second cleavage positions was maintained in *dcl1-9/dcl1-9* mutants (Fig. 5B). Therefore, we supposed that *dcl1-9* proteins processed pri-miR163 at an irregular position but could exactly measure 21 nt from the first cleavage position to the next position.

We thank the Salk Institute and *Arabidopsis* Biological Resource Center for providing the seeds for *dcl2-2* (SALK\_123586), *dcl3-1* (SALK\_005512), *dcl1-7* (*sin1-1*; stock number CS3089), and *dcl1-9* (*carpel factory*; stock number CS3828). This work was supported in part by Molecular Mechanisms of Plant-Pathogenic Microbe Interaction Grant-in-Aid 08680733 and Spatiotemporal Network of RNA Information Flow Grant-in-Aid 14035215 for scientific research, priority area (A), awarded by the Ministry of Education, Culture, Sports, Science, and Technology of Japan (to Y.W.).

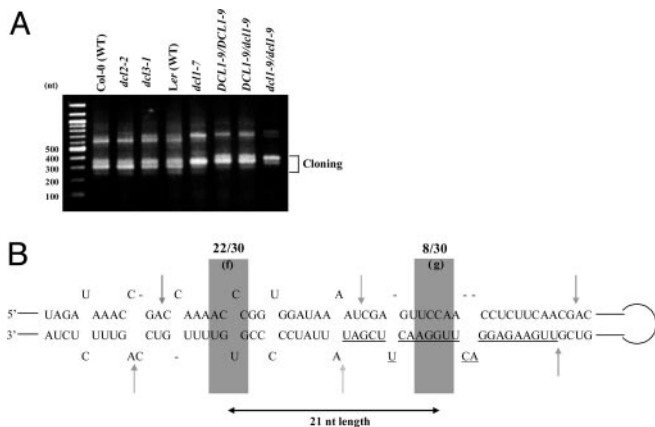


**Fig. 5.** Aberrant positioning of cleavage sites in the *dcl1-9* mutant. (A) Image of agarose gel electrophoresis of RT-PCR products. (B) The two cleavage sites in the *dcl1-9/dcl1-9* mutant. The gray boxes indicate the regions in which two cleavage sites extend. Zones f and g correspond to the roots of bands f and g of *dcl1-9/dcl1-9* mutants, respectively, shown in Fig. 4B. The number of sequenced clones corresponding to each site is indicated above each gray box. The gray arrows indicate the three cleavage sites in the wild type.

